Title
A MEASUREMENT OF THE COSMIC MICROWAVE BACKGROUND RADIATION TEMPERATURE AT 21 cm

Author
Levin, S.M.

Publication Date
1987-07-01

Lawrence Berkeley Laboratory
UNIVERSITY OF CALIFORNIA

Physics Division

Submitted to Astrophysical Journal

A Measurement of the Cosmic Microwave Background Radiation Temperature at 21 cm

S.M. Levin, C. Witebsky, M. Bensadoun, M. Bersanelli,
G. De Amici, A. Kogut, and G.F. Smoot

July 1987

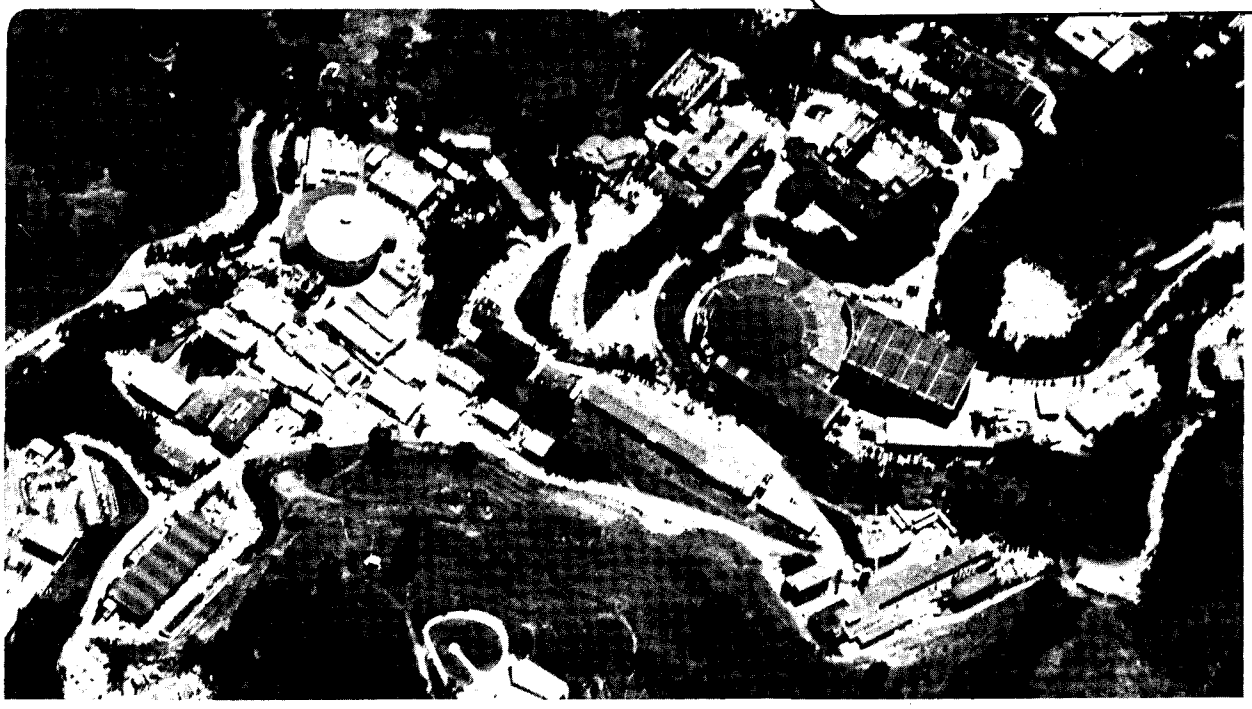

Prepared for the U.S. Department of Energy under Contract DE-AC03-76SF00098

DISCLAIMER

A Measurement of the Cosmic Microwave Background Radiation

Temperature at 21 cm

S.M. Levin, C. Witebsky, M. Bensadoun, M. Bersanelli, G. De Amici,

A. Kogut, and G.F. Smoot

Lawrence Berkeley Laboratory
University of California
and
Space Sciences Laboratory
University of California, Berkeley
Berkeley, California 94720

July 1987

A Measurement of the Cosmic Microwave Background Radiation Temperature at 21 cm

S. M. Levin, C. Witebsky, M. Bensadoun, M. Bersanelli, G. De Amici, A. Kogut, and G. F. Smoot

Lawrence Berkeley Laboratory and Space Sciences Laboratory,
University of California, Berkeley

ABSTRACT

We have measured the intensity of the cosmic microwave background radiation (CMBR) at a frequency of 1.410 GHz (21.26 cm wavelength), using a total-power radiometer. The brightness temperature of the CMBR at 1.410 GHz is 2.11±0.38 Kelvin at the 68% confidence level. The predominant sources of error are uncertainties in the reflection characteristics of the cold-load calibrator (0.03±0.31 K), subtraction of the signal from the galaxy (0.80±0.16 K), and the earth's atmosphere (0.83±0.10 K).

I. INTRODUCTION

The Cosmic Microwave Background Radiation (CMBR) is one of the few probes available to us to study the early history of the universe. For the most part, CMBR photons that reach us today have traveled undisturbed for 10 to 20 billion years. The CMBR taken as a whole may carry information from times as early as a year or two after the Big Bang.

In 1979, an international collaboration of researchers from Italy and the United States began an effort to make low-frequency measurements of the CMBR at frequencies of 2.5, 4.75, 10, 33, and 90 GHz (Smoot *et al* 1983, Smoot *et al.* 1985*a*, *b*) which substantially improved the limits on possible distortions of the CMBR spectrum.

The Berkeley group has continued the effort, making new measurements at 1.4, 3.7, 10, and 90 GHz in August of 1986 (Smoot *et al.* 1987*a*, De Amici *et al.* 1988 and Kogut *et al.* 1988). We report here on the measurement at 1.4 GHz.

II. CONCEPT OF THE EXPERIMENT

The basic experimental concept is to compare the microwave signal from the sky with the signal from a low-temperature target having known radiometric properties, then identify and subtract contributions from all sources other than the CMBR. To make this comparison, we use a radiometer, a device whose output voltage is proportional to the microwave power intercepted by its antenna.

Microwave signals are measured in antenna temperature, defined by

$$kT_A = \frac{dP}{d\nu}$$

where k is Boltzmann's constant, $\frac{dP}{d\nu}$ is the power received per unit bandwidth, and T_A is the antenna temperature. A blackbody at thermodynamic temperature T filling the aperture has an antenna temperature of

$$T_A = \frac{xT}{e^x - 1} \qquad (1)$$

where $x = h\nu/kT$, ν is the frequency, h is Planck's constant; at 1.410 GHz $h\nu/k$ has a value of 0.068 K .

As shown in Figure 1, there are a variety of signals which must be identified or eliminated in order to arrive at the antenna temperature of the CMBR. These include signals from the sun, the moon, the galaxy, the earth's atmosphere, man-made interference, contributions from the ground, from gravitational stresses, and from the low-temperature target. The signal difference between the sky and the low-temperature target is

$$G(S_{zenith} - S_{load}) = T_{A,zenith} - T_{A,load}$$

$$= T_{A,CMBR} + T_{A,gal} + T_{A,atm} + T_{A,ground} + \Delta T_{rad} - T_{A,load} \qquad (2)$$

where G is the radiometer's calibration coefficient; S_{zenith} is the radiometer output when viewing the zenith; S_{load} is the radiometer output when viewing the low-temperature target; $T_{A,zenith}$ is the antenna temperature of the sky as seen by the radiometer looking vertically; $T_{A,load}$ is the antenna temperature

of the low temperature target; $T_{A,CMBR}$ is the antenna temperature of the cosmic microwave background radiation; $T_{A,gal}$ is the antenna temperature of the galaxy; $T_{A,atm}$ is the antenna temperature of the atmosphere as seen by the 1.4 GHz radiometer observing the zenith; $T_{A,ground}$ is the contribution from the earth, picked up by diffraction in the antenna sidelobes; and ΔT_{rad} is any systematic change in the radiometer output caused by turning the radiometer over to view the low-temperature target. As determined by measurements made with the radiometer and a spectrum analyzer at the observing site, RFI was absent at the 10 mK level, so it is not included in Equation 2. Signals from the sun and the moon were eliminated simply by taking data only at night, at times when the moon is near or below the horizon, and are also absent from Equation 2. Solving for $T_{A,CMBR}$:

$$T_{A,CMBR} = G(S_{zenith} - S_{load}) - T_{A,gal} - T_{A,atm} - T_{A,ground} - \Delta T_{rad} + T_{A,load} . \quad (3)$$

III. THE INSTRUMENT AND EQUIPMENT

The radiometer collects radiation with a low-sidelobe, rectangular corrugated horn, made from aluminum sheet reinforced with aluminum angle (Witebsky *et al.* 1987). It is approximately 2 meters long, and separates into two sections (as shown in Figure 1) so that the radiometer can view the low-temperature calibration target.

Figure 2 shows a block diagram of the radiometer. A microwave signal entering the antenna passes through a waveguide-coaxial adaptor into a 3-stage GaAs FET amplifier, with 35 dB of gain. This is followed by a second amplifier, a bandpass filter to improve out-of-band RFI rejection, and a YIG bandpass filter. The YIG filter has a 25 MHz bandwidth and a center frequency which is set electronically, normally at either 1.410 GHz or 1.465 GHz. After the YIG filter is a third amplifier, and a square-law diode detector. The output of the detector is amplified and averaged by a d.c. integrating amplifier with a gain factor of 1000, and then sent through an analog-to-digital converter to a computer which records the data on magnetic disk.

Table 1 contains a summary of the radiometer characteristics and specifications. We measure the system noise temperature, T_{system}, by comparing the signal when the radiometer views the low-temperature target with the signal from an ambient-temperature target. The expected noise fluctuation for an integration time t is $\Delta T = \frac{T_{system}}{(Bt)^{1/2}}$, where B is the bandwidth (Tiuri and Raisanen 1986). The measured value given in Table 1 is based on the average variation of 2-second data samples taken with the radiometer at the observation site. The value and stability of G are determined by comparison of the signal from the ambient-temperature target with that from the low-temperature target at the time of the actual CMBR measurement. The radiometer is thermally controlled to improve gain stability; gain variation is dominated by drifts on a time scale of several minutes.

The low-temperature target (described in detail in Smoot *et al.* 1983 and Levin 1987) was kept cold with liquid helium (LHe), so that its signal was close to the signal received from the sky, minimizing the effects of gain calibration error. The radiometer made an RF-tight seal with the top of the LHe dewar by means

of an interface plate shaped to match the surfaces of both the radiometer and the dewar, with alignment pins for repeatability.

We measured the gain of the radiometer by comparing the signal from the low-temperature target with the signal from an ambient-temperature target, consisting of a low-reflection, temperature-monitored microwave absorber mounted in a thermally insulated cylindrical aluminum container.

IV. THE MEASUREMENT

In late July of 1986 we arrived at the Nello Pace Laboratory of the University of California's White Mountain Research Station, at an altitude of 3800 meters above sea level, on Mount Barcroft in the White Mountains near Bishop, California. After readying the support equipment and finishing preliminary testing of the radiometers, we began on August 8, 1986 to measure the CMBR temperature. We made measurements with the low-temperature target from 2:37 Universal Time (UT) to 3:32 UT, from 6:43 to 7:38 UT (while the galactic plane was nearly overhead) and from 10:35 until 11:30 UT. With the exception of the first few minutes over the low-temperature target, the following cycle was used for all data-taking runs:

1) The radiometer viewed the sky for 64 seconds.
2) The radiometer viewed the low-temperature target for 64 seconds
3) The radiometer viewed the sky again for 64 seconds
4) The radiometer viewed the ambient-temperature target for 64 seconds

This cycle was repeated throughout each run. Data were recorded in 16-second records, each consisting of eight 2-second data points. Moving the radiometer to view a different target always took less than 1 16-second record, and normally took less than 5 seconds.

On August 9, problems with the liquid helium (LHe) cooled low-temperature target resulted in an abnormally high rate of LHe loss, and the available measurement time was reduced. Measurements were made from 6:39 to 7:29 UT and from 10:08 to 11:02 UT.

V. ANALYSIS

In order to determine $T_{A,CMBR}$, we analyze each of the terms in Equation 3 separately.

a) $G(S_{zenith} - S_{load})$

During the 3 runs over the low-temperature target, 180 measurements were taken of S_{zenith} and S_{load} (Table 2). We ignore data from the 6 seconds immediately after the radiometer was moved. In addition, eight measurements have been rejected, as having anomalously high signal values, presumably caused by changing targets too slowly. Using the concurrently measured values of the calibration coefficient, the measured value of $G(S_{zenith} - S_{load})$ is -0.06 ± 0.03 Kelvin, where the error is based solely on the statistical fluctuations in the measurement, and assumes a Gaussian parent distribution. An increased variability in the radiometer output during the CMBR measurements, caused by small random changes in signal when the radiometer was moved or vibrated, indicates that some sensitivity to microphonics contributes to the statistical fluctuations.

The gain variation does not follow a Gaussian distribution, but in fact shows slow drifts (probably caused by temperature variation). The maximum spread between any 2 gain measurements is less than 5%, and the limit on gain saturation effects is less than 3% (as determined by inserting known attenuators in the amplification chain of the radiometer), so the error induced by gain variation is less than 0.005 K.

As shown in Figure 1, the radiometer observes the sky through an antenna extension which is not used for the LHe observations. Treating it as an uncorrugated antenna, we calculate the emission from the antenna extension to be less than 0.010 K at 1.410 GHz. The actual emission should comparable or smaller, because in a corrugated antenna the electric field falls to nearly zero at the E-plane walls, while in an uncorrugated antenna it remains constant. We therefore neglect emission from the antenna extension.

The final result for the first term in Equation 3 is

$$G(S_{zenith} - S_{load}) = -0.06 \pm 0.03 \text{ K.}$$

b) Absolute Reference Load

The antenna temperature of the low-temperature target, $T_{A,load}$, depends both on the power emitted by the low-temperature target, and on the power reflected from the low-temperature target. Based on the measured atmospheric pressure and the (less than 0.01 K) calculated emission from the reflective dewar walls, the power emitted by the LHe-cooled low-temperature target corresponded to an antenna temperature of 3.748±0.004 K.

Because the target was not a perfect absorber, a small fraction of the power emitted by the radiometer was reflected from the low-temperature target back into the antenna, and contributed to the antenna temperature of the low-temperature target. The power broadcast by the radiometer was equivalent to the 80 K system temperature. We measured the power reflection coefficient of the low-temperature target as viewed through the antenna, finding it to be -34 dB. Incoherent reflection thus contributed 0.030 K.

The 25 MHz bandwidth of the radiometer results in a 12-meter coherence length, which is longer than the length of the dewar, so that reflections from the low-temperature target can interfere coherently with reflections from inside the radiometer. Defining E_0^2 as the intensity of the power broadcast by the radiometer, the power reflected when viewing the low-temperature target is

$$E^2 = E_0^2 r_1^2 + E_0^2(1- r_1^2)r_2^2 + 2E_0^2(1- r_1^2) r_1 r_2 \cos(\Delta\Phi)$$

$$E^2 \approx E_0^2 r_1^2 + E_0^2 r_2^2 + 2E_0^2 r_1 r_2 \cos(\Delta\Phi) \qquad (4)$$

where r_1 is the magnitude of the amplitude reflection coefficient for reflections inside the radiometer, r_2 is the magnitude of the amplitude reflection coefficient for reflections from the target, $\Delta\Phi$ is the net phase difference between the two reflected signals when they recombine, and $r_1 << 1$.

The first term in Equation 4 does not affect the measurement, because it remains unchanged when comparing the signal from the sky with the signal

from the low-temperature target. The second term in Equation 4 represents the power reflected from the target when coherence effects are neglected, and is small. The final, phase-dependent term is the largest source of error, and is discussed below.

Using a directional coupler and a local oscillator, we measured the power reflection coefficient of the low-temperature target, the radiometer antenna, and the ambient-temperature target (Table 3). We also measured the input impedance of the radiometer by measuring reflection from a signal sent into the input of the first amplifier. Because the input impedance depended on the load seen by the radiometer, this measurement must be viewed somewhat skeptically.

To verify the phase-dependence of the last term in Equation 4, we temporarily removed the antenna and waveguide-to-coaxial adaptor, and caused the radiometer to view a shorted piece of coaxial line through an attenuator. We varied the phase by changing the length of the coaxial line, and varied the reflection coefficient by changing attenuators. As expected, the output of the radiometer varied sinusoidally with the phase of the reflected signal, and the amplitude of the variation indicated that the input impedance of the radiometer depended on the load.

Because CMBR data were taken at 1.465 GHz as well as at 1.410 GHz, we made reflection measurements at both frequencies. The radiometer was several times more sensitive to small reflections at 1.465 GHz than at 1.410 GHz, and we have therefore chosen to use only the 1.410 GHz data. Table 4 shows the amplitude of the sinusoidal variation with phase in the radiometer output for various values of reflection coefficient. For the 34 dB return loss of the low-temperature target at 1.410 GHz, the sliding short measurements indicate an upper limit of 0.9 K on the peak-to-peak variation, corresponding to an r.m.s. of 0.32 K for the phase dependent term.

When weather in the White Mountains permitted us to return, on June 14 and 15, 1987, we measured reflection effects without LHe cooling the target. By introducing additional cylindrical sections between the antenna and the target, we varied the effective phase of reflections from the target. From the variation in the radiometer signal when viewing the target with different

phase delays, we were able to place a 68% confidence level limit of 0.80 K on the signal variation with phase due to reflection from the target. The target temperature was 280 K during these measurements. As discussed in Appendix A, the reflection signal is proportional to the difference between the radiometer's broadcast temperature and the temperature of the target, so the equivalent phase-dependent variation for the LHe-filled target is 0.31 K. Since the phase is unknown, the correction applied is 0.00±0.31 K. Adding in the phase-independent term $(E_0^2\, r_2^2)$, the effect of reflections is to add 0.03±0.31 K to the antenna temperature of the target.

Thus, the total contribution from the cold calibration target is

$$T_{A,load} = 3.78 \pm 0.31 \text{ K}.$$

c) $T_{A,gal}$

The galactic contribution depends on the frequency of observation and on the part of the sky which is overhead when the CMBR is being measured. We used this spatial and frequency dependence to help determine $T_{A,gal}$.

At 1.410 GHz, radiation emitted by the galaxy is composed predominantly of synchrotron emission and thermal emission from HII regions near the galactic plane. Near the galactic plane, there is also a contribution from the HI line at 1.420 GHz. Figure 3 shows a model of the galactic signal at 1.410 GHz as a function of position on the sky, based on published maps of the galactic signal at 408 MHz (Haslam *et al.* 1982) and a compilation of known HII regions, neglecting contamination from the HI line and scaling the thermal and synchrotron emission by $\nu^{-2.10}$ and $\nu^{-2.75\pm0.1}$, respectively.

Data were taken (in roughly equal numbers) at right ascensions of $15^h\,52^m$ -- $16^h\,42^m$, $23^h\,53^m$ -- $00^h\,43^m$, and $23^h\,14^m$ -- $00^h\,04^m$. A brief measurement was also made at a right ascension of $20^h\,42^m$--$20^h\,46^m$, near the maximum galactic signal. From published measurements of the HI emission, appropriately scaled to the bandwidth and angular resolution of our radiometer, we calculate that

the measurement at $20^h\,42^m$--$20^h\,46^m$ includes a contribution of 0.3±0.1 K from the HI line at 1.420 GHz, and the HI contribution to the other measurements is less than 0.025 K (Kerr and Westerhout 1965, Burton 1976).

The measured difference between the galactic signal at $20^h\,42^m$--$20^h\,46^m$ and the average of the signal measured at other right ascensions is 2.3±0.2 K. Assuming an unknown (but spatially invariant) spectral index for the synchrotron emission and a spectral index of -2.1 for the thermal emission, and after subtracting the HI contamination, we can adjust the model shown in Figure 3 to match the measured signal difference. We find a spectral index of 2.79±0.15, and a galactic contribution of $T_{A,gal}$ = 0.80±0.16 K.

We can verify the estimate of $T_{A,gal}$ by comparing with a measurement recently made by G. Sironi at 0.60 GHz. According to his preliminary result (Sironi 1986), the galactic signal in a nearby (within 10 degrees) region of the sky at the same right ascension is $T_{A,gal,0.60\ \mathrm{GHz}}$ = 7±1 K. Scaling by $\nu^{-2.75\pm0.1}$, we find that at 1.410 GHz we have $T_{A,gal}$ = 0.67±0.15 K, which is consistent with the result above. The galactic signal used for substitution in Equation 3 is $T_{A,gal}$ = 0.80±0.16 K.

d) ΔT_{rad}

A major assumption of our measurement is that when the radiometer alternates between viewing the sky and viewing the low-temperature target, the only changes in signal are those due to the difference in targets. Conceivably, changes in the mechanical stresses on the electronic components could change the gain of the radiometer. Similarly, rotating the radiometer within the earth's magnetic field could have an effect on the magnetically sensitive components (particularly the YIG filter), again changing the gain of the radiometer.

Regardless of the causes, any change in the radiometer gain as a function of orientation can be detected by performing a test in which a target is attached to the horn of the radiometer, and the radiometer is repeatedly inverted, simulating the actual CMBR measurement. By measuring the amplitude of the

resultant square-wave modulation in the radiometer output, we can determine the extent to which inverting the radiometer changes its gain.

The ambient-temperature target is the only stable target capable of staying attached to the radiometer while being inverted, and was used as a target when doing flip tests. We soon discovered, however, that slight deformations in the shape of the target caused significant (~1 K) changes in the radiometer signal. After modification of the target to stiffen it and to reduce reflections, a vertical flip test showed the 1.410 GHz radiometer output to be 0.35 K higher when looking up at the ambient target than when looking down. The same test showed a -0.15 K effect at 1.465 GHz. The previously mentioned problems with the ambient target, as well as the strong frequency dependence of the effect, argue that the change seen is actually caused by a change in the reflection of the ambient-temperature target, masking any potential change in the radiometer gain. Using the signal seen in the flip test as an upper limit on changes in the radiometer gain due to gravitational stress, we thus have a possible systematic variation when viewing the ambient target of ±0.35 K. The effects of a gain change are proportional to $T_{target}+T_{system}$ so the possible effect of such gain changes on the CMBR measurement is 0.083 K.

A change in system temperature would not scale in this fashion, but one expects such a change to be accompanied by a corresponding change in gain. There are no active components upstream of the first amplifier, and a change in any component downstream from the first amplifier should result in a change in gain. A change in the insertion loss of the antenna would go undetected in a flip test with the ambient-temperature target, but the antenna is rigidly constructed and securely attached to the receiver to minimize any change due to gravitational stress. We therefore assume that the effect (if any) of rotating the radiometer is a change in gain, and take $\Delta T_{rad} = 0.00 \pm 0.083$ K.

e) $T_{A,ground}$

Because the surrounding terrain is at a temperature of ~300 K, and the sky signal is only ~4 K, the power per unit bandwidth radiated by the ground is nearly 100 times greater than the signal we are trying to detect. Accordingly, the antenna must have very low gain at angles below the local horizon. Figure 4 shows the measured antenna pattern as a function of angle in the H-plane at 1.410 GHz.

At its highest point, the local horizon for the observing site is 67 degrees from the zenith. Taking the antenna gain to be cylindrically symmetric with the gain as measured in the plane with poorer side-lobe rejection (the H-plane), and treating the effective ground temperature as 300 K for zenith angles greater than 60 degrees and 0 K for zenith angles less than 60 degrees, we have numerically integrated the antenna response, and conclude that (under these conservative assumptions) the signal received from the ground is $T_{A,ground} = 0.017 \pm 0.008$ K. The assumptions of beam symmetry and uniform horizon height, although invalid, are conservative, and the resulting value for $T_{A,ground}$ is so small compared to other sources of uncertainty that further analysis is not justified.

f) $T_{A,atm}$

At the same time the 1.4 GHz radiometer was taking data, radiometers at 90 GHz, 10 GHz, and 3.7 GHz were making atmospheric measurements from the same high-altitude site (Smoot *et al.* 1987*a*, Kogut *et al.* 1988, De Amici *et al.* 1988). We have extrapolated the atmospheric measurements from 3.7 GHz to 1.410 GHz, based on published models of the frequency dependence of atmospheric absorption (Rosenkranz 1975, Waters 1976, Liebe 1981, Costales *et al.* 1986).

According to the atmospheric models and the measurements at 90 GHz, the atmospheric emission at 1.410 GHz ranges from 93% of the emission at 3.7 GHz

(an atmosphere with 8 mm of water vapor) to 97% of the emission at 3.7 GHz (a completely dry atmosphere). Thus the ratio of the atmospheric emission at 1.410 GHz to the emission at 3.7 GHz is 0.95±0.02. Extrapolating from the 0.870±0.108 K antenna temperature of the vertical atmosphere at 3.7 GHz (De Amici *et al.* 1988), the antenna temperature of the vertical atmosphere at 1.410 GHz is $T_{A,atm}$ = 0.83±0.10 K.

To confirm the result of the extrapolation from measurements at 3.7 GHz, we have performed the analogous extrapolation from atmospheric measurements at 10 GHz . The measured value of $T_{A,atm}$ at 10 GHz is 1.2±0.1 K (Kogut *et al.* 1988), and the ratio of atmospheric emission at 1.410 GHz to the atmospheric emission at 10 GHz is 0.70±0.13, so extrapolating from the 10 GHz measurement yields $T_{A,atm}$ = 0.84±0.15 K at 1.410 GHz, in excellent agreement with the previous estimate.

The value adopted for substitution in Equation 3 is $T_{A,atm}$ = 0.83±0.10 K.

VI. RESULTS AND CONCLUSIONS

Table 5 summarizes the systematic errors discussed in the previous section. Summing all the terms and adding the errors in quadrature, we arrive at the antenna temperature of the CMBR at 1.410 GHz:

$$T_{A,CMBR} = 2.08\pm0.37 \text{ K}$$

Converting to brightness temperature (Equation 1), we have the final result:

$$T_{CMBR} = 2.11\pm0.38 \text{ K}$$

at the 68% confidence level. While there are no other recent measurements of T_{CMBR} near 1.4 GHz, Penzias and Wilson (1967) reported T_{CMBR} = 3.2±1.0 K at

1.42 GHz, and Howell and Shakeshaft (1966) reported $T_{CMBR} = 2.8 \pm 0.6$ K at 1.45 GHz.

All of the recent measurements at wavelengths longer than 0.11 cm are consistent at the 68% confidence level with a blackbody CMBR spectrum of temperature 2.74 ± 0.02 K. Detailed analysis of the possible implications of recent measurements of T_{CMBR} is given in Smoot *et al.* 1987*b*.

ACKNOWLEDGEMENTS

We thank Jon Aymon, John Gibson, Larry Levin, Faye Mitschang, and Carol Stanton for their assistance. The staff of the White Mountain Research Station was a tremendous help, as usual. This work was supported in part by NSF Grant No. AST 8406187, and by the Department of Energy under Contract DE-AC0376SF00098. We thank ISTRA (Istituto Studi per la Transizione) Milano and Fondazione A. Gini of Padova for fellowship support of M. Bersanelli.

APPENDIX

REFLECTION EFFECTS

We will consider reflection effects for a radiometer observing an optically thick target. Without loss of generality, we can describe the system as an ideal radiometer on one side, an ideal absorber on the other side, and two sources of reflection in between. One source of reflection represents the combination of all reflections which take place inside the physical radiometer, and the other source represents all reflection effects from the physical target. Reflection effects involve reflection of the signal emitted by the target, as well as of the signal emitted by the radiometer. If the reflection is symmetric with respect to direction, as is the case for any system without non-reciprocal elements, the same fraction of power is reflected back to the target as was reflected back to the radiometer (Ramo *et al.* 1965). Thus, if the fractional power reflected back to the receiver is $\frac{|E_{Rr}|^2}{|E_R|^2}$, then the fractional power from the absorber transmitted through to the radiometer will be

$$\frac{|E_{At}|^2}{|E_A|^2} = \frac{|E_A|^2 - |E_{Ar}|^2}{|E_A|^2} = 1 - \frac{|E_{Ar}|^2}{|E_A|^2} = 1 - \frac{|E_{Rr}|^2}{|E_R|^2}$$

where the subscripts A, R, r, and t refer to the absorber, the receiver, the reflected component, and the transmitted component, respectively. Because the radiation emitted by the radiometer is incoherent with the radiation emitted by the target, we can treat the two reflection problems separately, and simply add the power which arrives at the radiometer input after being emitted by the target to the power which arrives there after being emitted by the radiometer and reflected. The signal received by the radiometer is

$$|E_{At}|^2 + |E_{Rr}|^2 = |E_A|^2 - |E_A|^2\frac{|E_{Rr}|^2}{|E_R|^2} + |E_{Rr}|^2$$

$$= |E_A|^2 - \frac{|E_{Rr}|^2}{|E_R|^2}\left(|E_A|^2 - |E_R|^2\right).$$

The net reflection effect will therefore be proportional to the difference between the radiometer's broadcast temperature (~80 K) and the temperature of the target.

When the target is at LHe temperature (~4 K), the decrease in target emission is small, but when the emission temperature is the ambient temperature, 280 K, the net reflection effect scales by a factor of

$$(280\ \text{K} - 80\ \text{K})/(4\ \text{K} - 80\ \text{K}) = -2.6.$$

TABLES

TABLE 1

RADIOMETER CHARACTERISTICS

T_{system}	80±3 K	
Sensitivity	0.017 K/$\sqrt{\text{Hz}}$	(theoretical)
	0.023 K/$\sqrt{\text{Hz}}$	(measured)
Calibration Coefficient	46 K/V	
Gain Variation	<0.1 %/minute	
Operating Frequency	1.410 GHz	(adjustable)
Bandwidth	0.025 GHz	

TABLE 2

MEASUREMENTS OF SKY TEMPERATURE MINUS LHe TEMPERATURE

	# OF PTS.[a] (removed)	AVE. (K)	RMS (K)	σ (K)
August 8, 1986				
1st run	57 (1)	-0.027	0.428	0.057
2nd run	60 (1)	+0.005	0.271	0.035
August 9, 1986				
1st run	63 (6)	-0.160	0.516	0.065

[a] Each point represents the difference between two 16-second records.

TABLE 3

POWER REFLECTION COEFFICIENTS

Target	Return Loss[a] 1 MHz BW[b]	25 MHz BW[c]
low-temperature calibrator	-44 dB	-34 dB
ambient-temp. calibrator	-27 dB	-27 dB
antenna (sky)	-30 dB	-29 dB
antenna extension	-39 dB	-38 dB
input to 1st amplifier (sensitive to load)	-(22 dB)	-(22 dB)

[a]Measured with the directional coupler and spectrum analyzer.
[b]Return loss given for the 1 MHz resolution of the measurement.
[c]Return loss averaged over 25 MHz, to approximate the radiometer's bandwidth.

TABLE 4

RADIOMETER RESPONSE TO REFLECTION PHASE VARIATION

Frequency (GHz)	Attenuator	Equivalent Return Loss	Peak-Peak Amplitude
1.410	16 dB	32 dB	< 0.9 K
1.410	10 dB	20 dB	16 K
1.410	6 dB	16 dB	22 K
1.410	0 dB	0 dB	33 K
1.465	16 dB	32 dB	6 K
1.465	10 dB	20 dB	9 K
1.465	6 dB	12 dB	28 K

TABLE 5

TERMS CONTRIBUTING TO CMBR MEASUREMENT

$G(S_{zenith} - S_{load})$	-0.06 ± 0.03[a]	K
$T_{A,load}$	3.78 ± 0.31	K
$T_{A,gal}$	0.80 ± 0.16	K
$T_{A,atm}$	0.83 ± 0.10	K
ΔT_{rad}	0.000 ± 0.083	K
$T_{A,ground}$	0.017 ± 0.008	K

[a] All errors are quoted at the 68% confidence level.

REFERENCES

Burton, W.B. 1976 *Ann. Rev. Astron. Astrophys.*, **14**, 275-306.

Costales, J., *et al.* 1986, *Radio Science*, **21**, 47.

De Amici, G., Smoot, G., Aymon, J., Bersanelli, M., Kogut, A., Levin, S., and Witebsky, C. 1988, *Ap. J.* (in press).

Haslam, C.G.T., Salter, C.J., Stoffel, H., and Wilson, W.E. 1982, *Astr. Astroph. Suppl. Ser.*, **47**, 1.

Howell, T.F. and Shakeshaft, J.R. 1966, *Nature*, **210**, 1318.

Kerr, F. J. and Westerhout, G. 1965, "Distribution of Interstellar Hydrogen" in *Galactic Structure*, Blaauw, A. and Schmidt, M., Ed. U. of Chicago Press, Chicago, Ill..

Kogut, A., *et al.* 1988, *Ap. J.* (February 1 issue).

Levin, S. 1987, PhD Dissertation, U. C. Berkeley, LBL#23302

Liebe, H.J. 1981, *Radio Science*, **16(6)**, 1183.

Penzias, A.A., and Wilson, R.W. 1965, *Ap. J.*, **142**, 419.

Penzias, A.A., and Wilson, R.W. 1967, *Astron. J.*, **72**, 315.

Ramo, S., Whinnery, J. R., Van Duzer, T. 1965, *Fields and Waves in Communication Electronics*, 589-611, Wiley & Sons, Inc., New York.

Rosenkranz, P. W. 1975, *IEEE Trans. Antennas Propagation*, **AP-23(4)**, 498.

Sironi, G. 1986, priv. comm.

Smoot, G., *et al.* 1983, *Phys. Rev. Letters*, **51**, 1099

Smoot, G., *et al.* 1985*a*, Conference Proceedings, *Societa' Italiana di Fisica*, **1**, 27.

Smoot, G., *et al.* 1985*b*, *Ap. J. Lett.*, **291**, L23.

Smoot et al. 1987*a*, *Ap. J. Lett.*, **317**, L45-L49.

Smoot et al. 1987*b*, submitted to *Ap. J.*

Tiuri, M. and Raisanen, A. 1986, "Radio-Telescope Receivers" in *Radio Astronomy*, 2nd edition, J. D. Kraus, Ed. Cygnus-Quasar Books, Powell, Ohio.

Waters, J. R. 1976, "Absorption and Emission by Atmospheric Gases," in *Methods of Experimental Physics*, vol. **12B**, Ed. M. L. Meeks, Academic Press, NY.

Witebsky, C., Smoot, G. F., Levin, S., and Bensadoun, M. 1987, *IEEE Antennas and Propagation* (in press November issue).

FIGURE CAPTIONS

Figure 1. Concept of the experiment. The radiometer is alternately pointed at the sky and at the cryogenic calibration target. After comparing the signal from the sky with the signal from the target, sources of radiation other than the CMBR are identified and subtracted.

Figure 2. Block diagram of the 1.4 GHz radiometer.

Figure 3. Galactic signal as a function of right ascension as seen from the observing site (latitude 38 degrees North), extrapolated from published measurements at 0.4 GHz (Haslam *et al.* 1982) as well as thermal HII emission. HI emission is not shown. The upper, middle, and lower curves correspond to synchrotron spectral indices of 2.65, 2.75, and 2.85, respectively. The arrows indicate right ascensions at which measurements were made.

Figure 4. Gain pattern of the antenna in the H-plane at 1.410 GHz. The apparent rise in gain at angles greater than 160 degrees may be due to reflection from objects in the test range where the gain pattern was measured.

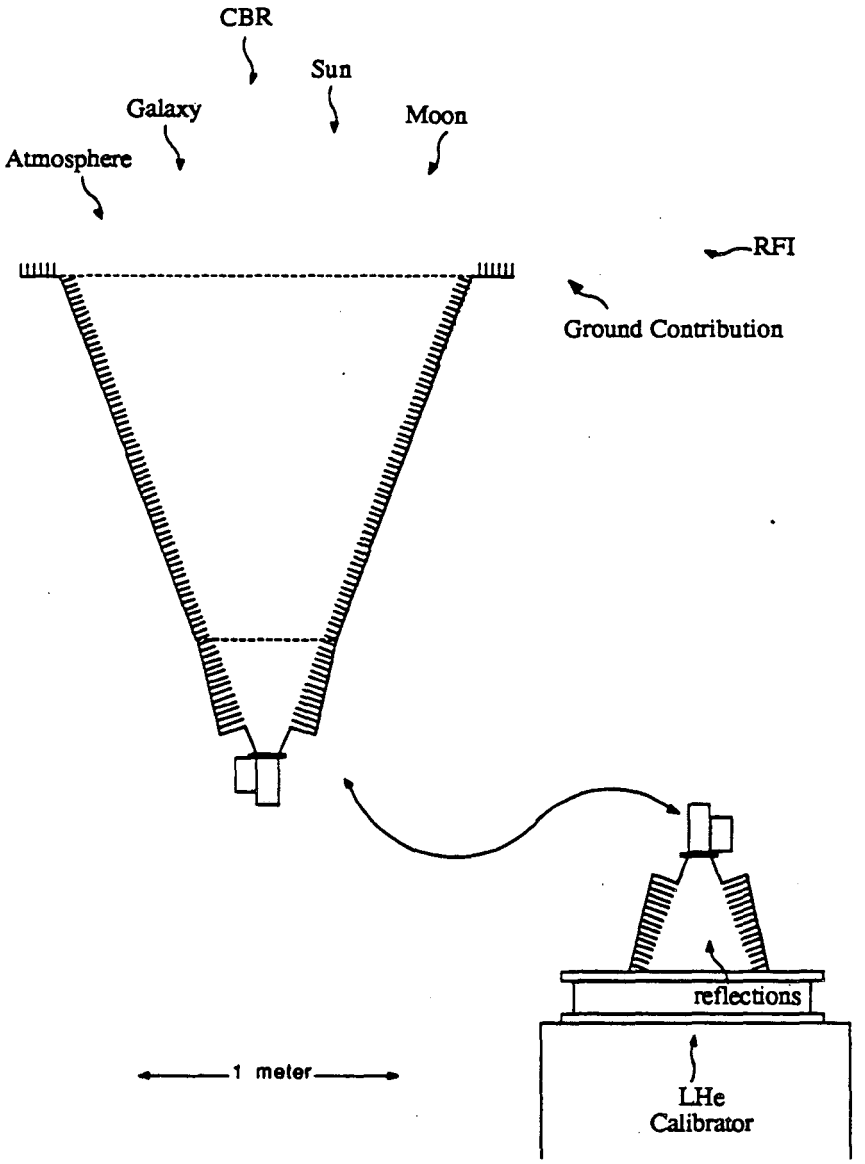
CBR
Sun
Galaxy
Moon
Atmosphere
RFI
Ground Contribution
reflections
1 meter
LHe
Calibrator

Fig. 1

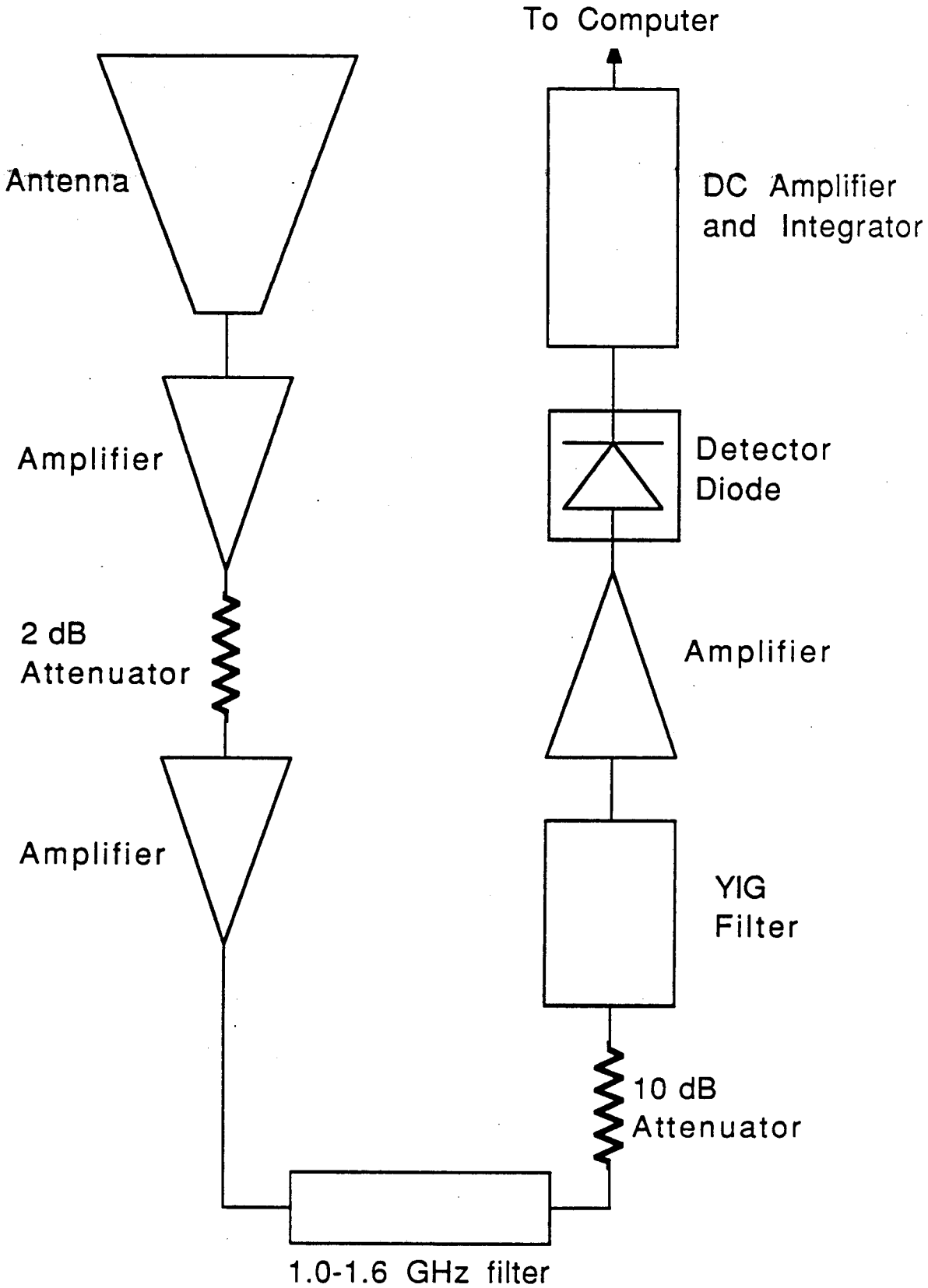
To Computer
Antenna
DC Amplifier
and Integrator
Amplifier
Detector
Diode
2 dB
Attenuator
Amplifier
Amplifier
YIG
Filter
10 dB
Attenuator
1.0-1.6 GHz filter

Fig. 2

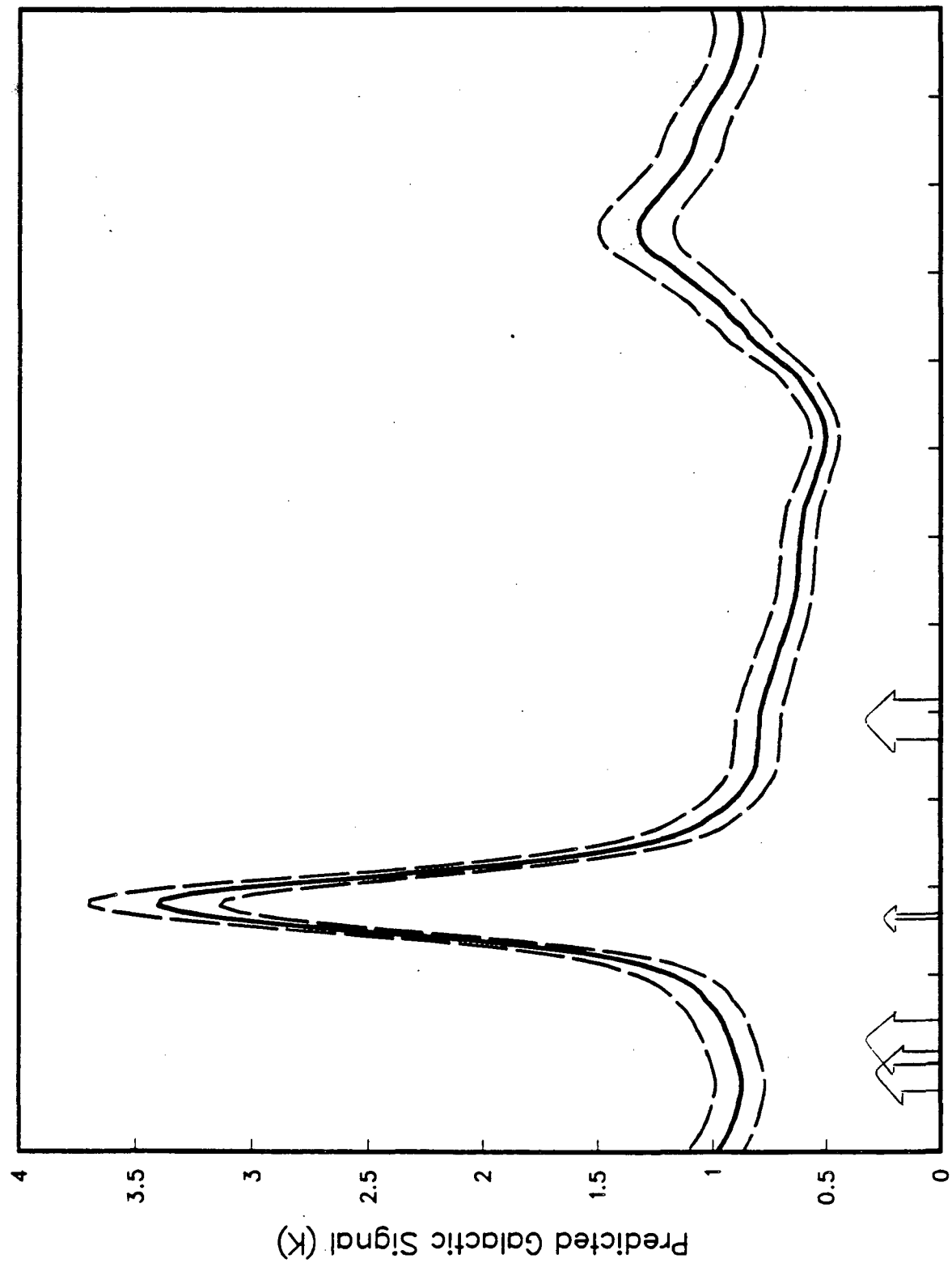
Predicted Galactic Signal (K)
0
0.5
1
1.5
2
2.5
3
3.5
4
24
22
20
18
16
14
12
10
8
6
4
2
Right Ascension (hours)

Fig. 3

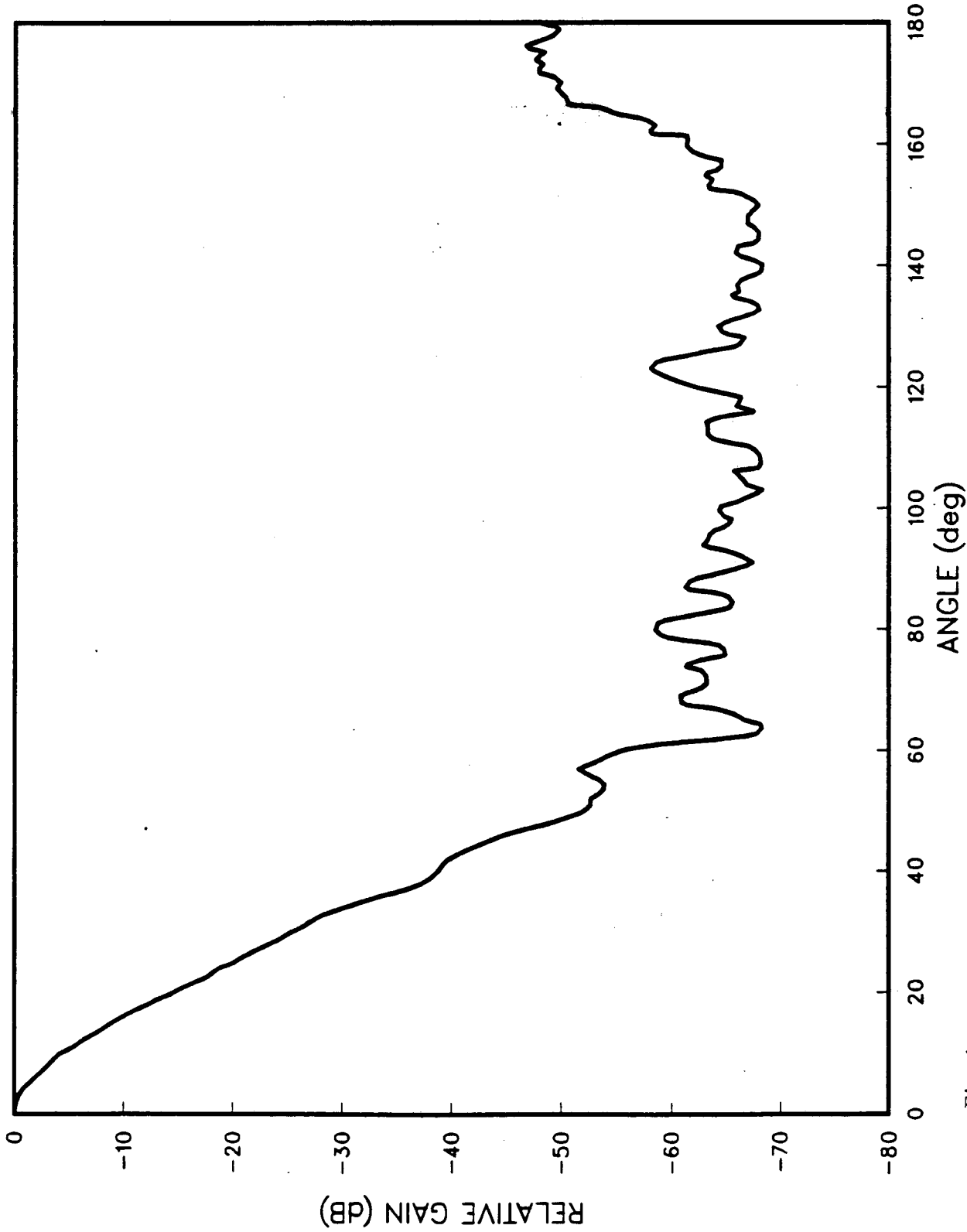
RELATIVE GAIN (dB)
0
-10
-20
-30
-40
-50
-60
-70
-80
0
20
40
60
80
100
120
140
160
180
ANGLE (deg)

Fig. 4

LAWRENCE BERKELEY LABORATORY
TECHNICAL INFORMATION DEPARTMENT
UNIVERSITY OF CALIFORNIA
BERKELEY, CALIFORNIA 94720